Optical Engineering

SPIEDigitalLibrary.org/oe

Beam wander analysis for focused partially coherent beams propagating in turbulence

Xifeng Xiao
David G. Voelz

SPIE

Beam wander analysis for focused partially coherent beams propagating in turbulence

Xifeng Xiao
David G. Voelz
New Mexico State University
Klipsch School of Electrical and Computer Engineering
Las Cruces, New Mexico 88003
E-mail: davvoelz@nmsu.edu

Abstract. We extend the theory of beam wander for propagation through atmospheric turbulence to the case of a focused partially coherent beam (PCB). In addition to investigating the beam wander expression, we restate expressions for the beam size, long- and short-time average beam intensity profile, and the on-axis scintillation index of tracked and untracked beams. A wave optics simulation is implemented and the numerical results are compared with corresponding analytic results. The cases examined involve turbulence strengths ranging from $C_n^2 = 10^{-16}$ to 10^{-14} $m^{-2/3}$ and for various horizontal paths ranging from 1 to 10 km. Although the extended analytic theory stems from a study of coherent beams, the simulation results show good agreement with the analytical results for PCBs in fluctuation regimes ranging from weak to intermediate.
 [DOI: 10.1117/1.OE.51.2.026001]

Subject terms: free-space optics; laser communication; focused partially coherent beam; wave optics simulation; beam wander; tracked beam; untracked beam; atmospheric turbulence.

Paper 111264 received Oct. 11, 2011; revised manuscript received Dec. 26, 2011; accepted for publication Dec. 28, 2011; published online Mar. 1, 2012.; corrected Mar. 21, 2012.

1 Introduction

Beam wander refers to the gross displacement of an optical beam intensity pattern relative to the pattern for an ideal (vacuum) propagation. Beam wander behavior and related attributes, such as root mean square (RMS) centroid and scintillation index, are important performance indicators of optical beams propagating through turbulence.[1–3] These beam characteristics have been studied extensively by many researchers over the last five decades through different approaches and for a variety of beam types.[4–8] The beam wander of a single ray was examined by Beckmann and Chernov using a geometrical optics (GO) approximation.[4,9] An expression for the wander of a Gaussian beam was first developed using a Huygens–Fresnel approach,[5] and later was derived by applying a Markovian random process approximation and Ehrenfest's theorem from quantum mechanics.[10,11] Eyyuboglu, Cil, and Baykal evaluated the beam wander behavior for several different beam types such as dark-hollow, flat-topped, annular, cos, and cosh-Gaussian beams.[12,13] Beam wander effects for a spatially PCB were investigated by Berman et al., who introduced a photon distribution function method.[14] To the best of our understanding, the effect of an average phase curvature applied to the PCB, for example "focus," was not included in the study.

Recently, Andrews and Phillips developed expressions for the beam wander of a focused coherent Gaussian beam in a weak fluctuation turbulence regime by applying Rytov theory.[15] Subsequently, Recolons et al. compared the theoretical models with simulations, and satisfactory agreement was observed.[16] In terms of free space optical (FSO) applications, a convergent PCB or a PCB with some other specified wavefront curvature can greatly improve link performance.[17] However, a convergent beam can still have a significant wander component. This brings us to the question: How does a focused PCB wander when propagating through turbulence?

In this paper, we extend the beam wander theory of Andrews and Phillips to include the focused PCB case. We examine the beam wander (RMS beam centroid) behavior and, in addition, investigate the beam size, the scintillation index, and the mean intensity patterns for both tracked and untracked beams. For validation purposes, a numerical wave optics simulation (WOS) is implemented to create focused PCBs and model their propagation through turbulence. Results are presented and compared with the analytic models for scenarios with turbulence strength varying from weak to strong and propagation distances ranging from 1 to 10 km.

2 Beam Wander Theory

2.1 *Beam Wander Variance*

Beam wander can be characterized by the transverse movement r_c of the "hot spot" within the beam profile. The general expression of the beam wander variance, $\langle r_c^2 \rangle$, was modeled by Andrews and Phillips as:[15]

$$\langle r_c^2 \rangle = 4\pi^2 k^2 W^2(Z) \int_0^Z \int_0^\infty \kappa \Phi_n(\kappa) H_{\mathrm{LS}}(\kappa, z) \times [1 - e^{-\Lambda_P Z \kappa^2 (1 - z/Z)^2 / k}] \mathrm{d}\kappa \mathrm{d}z, \quad (1)$$

where κ is the spatial wave number, k is the optical wave number defined by $k = 2\pi/\lambda$ and λ is the wavelength. Z is the propagation distance from the transmitter to the receiver, and z is a distance variable that ranges from 0 to Z. The parameter Λ_P is defined and discussed below. $H_{\mathrm{LS}}(\kappa, z)$ is a filter function that selects the low spatial frequencies in the

turbulence power spectrum $\Phi_n(\kappa)$ that correspond to large spatial scales. In our work the filter function was applied in the same manner for all turbulence regimes, weak through strong. The filter function can be expressed as

$$H_{\mathrm{LS}}(\kappa, z) = \exp[-\kappa^2 W^2(z)], \tag{2}$$

where $W(z)$ is the free space beam radius (or beam size) at distance z. For a focused PCB with an initial beam size W_0, a phase-front curvature F and coherence length l_c, we have[18,19]

$$W(z) = W_0\left[\left(1-\frac{z}{F}\right)^2 + \left(1+\frac{2W_0^2}{l_c^2}\right)\left(\frac{2z}{kW_0^2}\right)^2\right]^{1/2}. \tag{3}$$

The coherence length l_c is a measure of the transverse spatial correlation of the beam source field. When l_c is on the order of W_0, the effect on the beam size can be significant. l_c is infinite for a perfectly coherent beam.

Returning to Eq. (1), we now define the nondimensional output beam parameter Λ_P of a PCB, and it can be written as

$$\Lambda_P = \frac{2Z}{kW^2(Z)}. \tag{4}$$

Typically,$\Phi_n(\kappa)$ in Eq. (1) is assumed to be the Kolmogorov spectrum, which is defined as

$$\Phi_n(\kappa) = 0.033 C_n^2 \kappa^{-11/3}, \tag{5}$$

where C_n^2 is the refractive index structure parameter and is assumed to be constant for horizontal propagation. Apply the geometrical optics (GO) approximation and the last term in Eq. (1) becomes:

$$1 - e^{-\Lambda_P Z\kappa^2(1-z/Z)^2/k} \approx \frac{\Lambda_P Z\kappa^2(1-z/Z)^2}{k},$$
$$\text{if } \frac{\Lambda_P Z\kappa^2}{k} \ll 1. \tag{6}$$

Inserting Eq. (6) into Eq. (1) and calculating the integrations, we obtain the beam wander variance:[15]

$$\langle r_c^2\rangle = 7.25 C_n^2 Z^3 W_0^{-1/3}\int_0^Z \left(1-\frac{z}{Z}\right)^2 G_P(z)^{-1/6}\mathrm{d}z, \tag{7}$$

where $G_P(z)$ is a function defined for the focused PCB beam as

$$G_P(z) = [W(z)/W_0]^2. \tag{8}$$

For coherent beams, the second term in the bracket of the definition for $W(z)$ [Eq. (3)] is typically negligible and is often dropped to simplify the calculation of $G_P(z)$[15]. For PCBs, this term could be significant and cannot be ignored. A closed-form analytic solution of Eq. (7) with Eq. (8) included is attainable and involves a hypergeometric function that is typically evaluated numerically. For the results in this paper, we bypass this step and simply evaluate Eq. (7) directly using numerical integration.

2.2 *Mean Intensity Profiles*

Consider a beam with the field $U(r, z)$, where r is the transverse distance from the beam center in the plane perpendicular to the propagation direction. For a unit-amplitude field at the source plane ($z = 0$), we have:

$$U(r, 0) = \exp\left(-\frac{r^2}{W_0^2} - i\frac{kr^2}{2F}\right)\exp[i\xi(r, 0)], \tag{9}$$

where $\xi(r, 0)$ is the random phase function to characterize the partially coherent beam at the beam source ($z = 0$) with parameter l_c. As the beam propagates through turbulence, assuming the average intensity profile at the receiver is Gaussian,[20,21] the only free parameter that governs the beam profile is the receiving beam size/radius. Following Fante, who considered long-time (LT) and short-time (ST) averages, which correspond to untracked and tracked beams, respectively, the respective beam size values, $W_{\mathrm{LT}}(Z)$ and $W_{\mathrm{ST}}(z)$, are related by:[6]

$$W_{\mathrm{ST}}^2(Z) = W_{\mathrm{LT}}^2(Z) - \langle r_c^2\rangle, \tag{10}$$

where $\langle r_c^2\rangle$ is the beam wander variance. Expressions for $W_{\mathrm{LT}}(Z)$ have been developed in several recent publications. We compared expressions presented by Andrews and Phillips, Ricklin and Davidson, and Korotkova et al. for the LT average beam size and irradiance distribution, and found that for a coherent Gaussian beam propagated over a relatively short distance and/or through weak turbulence, the theories from these authors[15,22,23] are almost identical and are consistent with our wave optics simulation results. However, for propagation through stronger turbulence, the theory put forward by Ricklin and Davidson provides a better fit to our simulation results. This expression for the LT average beam size is given by:[22]

$$W_{\mathrm{LT}}(Z) = W_0\left[\left(1-\frac{Z}{F}\right)^2 + \left(1+\frac{2W_0^2}{l_c^2}+\frac{2W_0^2}{\rho_0^2}\right)\left(\frac{2Z}{kW_0^2}\right)^2\right]^{1/2}, \tag{11}$$

where ρ_0 is defined as the coherence length of a spherical wave propagating in turbulence and is given by

$$\rho_0 = (0.55 C_n^2 k^2 Z)^{-3/5}. \tag{12}$$

Consequently, the mean intensity profiles of the LT and ST beams at the receiver, $I_{\mathrm{LT}}(r, Z)$, and $I_{\mathrm{ST}}(r, z)$, can be written as:[15,22]

$$I_{\mathrm{LT}}(r, Z) = \frac{W_0^2}{W_{\mathrm{LT}}^2(Z)}\exp\left[-\frac{2r^2}{W_{\mathrm{LT}}^2(Z)}\right], \tag{13}$$

and

$$I_{\mathrm{ST}}(r, Z) = \frac{W_0^2}{W_{\mathrm{ST}}^2(Z)}\exp\left[-\frac{2r^2}{W_{\mathrm{ST}}^2(Z)}\right]. \tag{14}$$

2.3 *Scintillation Theory (On-Axis)*

To be consistent with previous work on scintillation, we use the terms "tracked" for ST average results and "untracked"

for LT average results in this section. The derivations of the on-axis scintillation indices of tracked and untracked coherent beams have been thoroughly discussed in several papers listed in Refs. 8 and 15. Corresponding analytical expressions for a focused PCB beam are found by incorporating the PCB beam size formulation. For a tracked beam, the on-axis scintillation index in weak turbulence is given by

$$\sigma_{I,\mathrm{tr,weak}}^2(Z) = 3.86\sigma_R^2\left\{0.4[(1+2\Theta_P)^2+4\Lambda_P^2]^{5/12} \times \cos\left[\frac{5}{6}\tan^{-1}\left(\frac{1+2\Theta_P}{2\Lambda_P}\right)\right] - \frac{11}{16}\Lambda_P^{5/6}\right\}, \quad (15)$$

where Θ_P is a nondimensional PCB output beam parameter given by

$$\Theta_P = \frac{1-\frac{Z}{F}}{\left(1-\frac{Z}{F}\right)^2+\left(\frac{2Z}{kW_0^2}\right)^2\left(1+\frac{2W_0^2}{l_c^2}\right)}, \quad (16)$$

and $\sigma_R{}^2$ is the Rytov variance given by

$$\sigma_R^2 = 1.23C_n^2k^{7/6}Z^{11/6}. \quad (17)$$

For an untracked beam, the on-axis scintillation index is

$$\sigma_{I,\mathrm{un,weak}}^2(Z) = 4.42\sigma_R^2\Lambda_P^{5/6}\frac{\sigma_{\mathrm{pe}}^2}{W^2(Z)} + \sigma_{I,\mathrm{tr}}^2(Z), \quad (18)$$

where $\sigma_{\mathrm{pe}}{}^2$ is the jitter-induced pointing error variance. For a focused PCB beam

$$\sigma_{\mathrm{pe}}{}^2 = 7.25C_n^2Z^3W_0^{-1/3}\int_0^Z\left(1-\frac{z}{Z}\right)^2\left\{\left[\frac{1}{G_P(z)}\right]^{1/6} - \left[\frac{K_r^2W_0^2}{1+K_r^2W_0^2G_P(z)}\right]^{1/6}\right\}\mathrm{d}z, \quad (19)$$

where

$$K_r = \frac{2\pi}{2.1\rho_0}. \quad (20)$$

Equations (15) and (18) are restricted to weak turbulence. Under intermediate to strong turbulence, we follow the theory developed by Andrews and Phillips,[15] which yields the general expression for the scintillation index for a tracked beam

$$\sigma_{I,\mathrm{tr}}^2(Z) = \exp\left\{\frac{0.49\sigma_{I,\mathrm{tr,weak}}^2(Z)}{[1+0.56(1+\Theta_P)\sigma_{I,\mathrm{tr,weak}}^{12/5}(Z)]^{7/6}} + \frac{0.51\sigma_{I,\mathrm{tr,weak}}^2(Z)}{[1+0.69\sigma_{I,\mathrm{tr,weak}}^{12/5}(Z)]^{5/6}}\right\} - 1, \quad (21)$$

and for an untracked beam

$$\sigma_{I,\mathrm{un}}^2(Z) = 4.42\sigma_R^2\left(\frac{2Z}{k}\right)^{5/6}\frac{\sigma_{\mathrm{Pe}}^2}{W_{\mathrm{LT}}^{11/3}(Z)} + \sigma_{I,\mathrm{tr}}^2(Z). \quad (22)$$

3 Wave Optics Simulations

Comparison of analytic values with numerical WOS results helps validate both the theory and simulation modeling approaches. In addition, the numerical approach can help verify that the GO approximation used in the analytic result is acceptable. The WOS approach has been discussed in detail in various publications.[24–26] For a focused PCB simulation we follow the approach developed for a collimated PCB but with a phase curvature term applied at the source plane.[27–29] Specifically, the implementation procedure can be described as follows: (1) generate a random phase screen with appropriate spatial coherence length l_c;[29] (2) apply the phase screen to a coherent beam in the source plane; (3) numerically "propagate" the beam to the observation plane[28] through a separate set of phase screens that model atmospheric turbulence and compute the intensity; and (4) repeat steps 1 to 3 N_{PS} times, each time with a different realization of the spatial coherence screen (but without changing the turbulence screen realizations) and average the intensity at the observation plane. The average intensity is the PCB result. We typically limit N_{PS} to 30 to reduce computation time.

Atmospheric turbulence is simulated with a split-step approach involving a series of random screens evenly spaced along the propagation path.[30] Our turbulence screens assume a Kolmogorov spectrum. The number of turbulence screens (N_{TS}) used for a particular scenario is determined following the criteria described in Ref. 24. For each data point presented, 500 propagations are simulated through different realizations of turbulence, which means a total of $N_{\mathrm{PS}} \times N_{\mathrm{TS}} = 30 \times 500 = 15,000$ propagations are required for each point. Both LT (untracked) and ST (tracked) cases are investigated. For ST (tracked) results, the beam centroid for each of the 500 turbulence realizations is found and each intensity pattern is translated to the center of the numerical grid before the measures are computed. The WOS program codes were implemented in the MATLAB environment.

The link parameters for results presented in this paper are listed in Table 1. The analysis and simulations can be applied to wide range of parameters, but the choices here are characteristic of moderate-length terrestrial links (1 to 10 km) in weak ($\sigma_R^2 < 1$) to strong ($\sigma_R^2 > 1$) intensity fluctuation regimes. The phase curvature parameter F is set equal to the propagation distance Z so the effect of focus over a range of distances can be investigated. PCB coherence lengths of 2 and 5 cm are typical of values that provide near-optimal link performance in applications like FSO communications.[17]

Table 1 WOS simulation parameters for link scenarios studied in this paper.

Scenario parameters	C_n^2	σ_R^2	N_{TS}
$W_0 = 5$ cm, $\lambda = 1$ μm, $Z = 1$ to 10 km, $F = Z$, $l_c = 2$ or 5 cm	10^{-16} m$^{-2/3}$	0.003 to 0.23	2
	10^{-15} m$^{-2/3}$	0.03 to 2.3	2 to 6
	10^{-14} m$^{-2/3}$	0.3 to 22.7	2 to 20

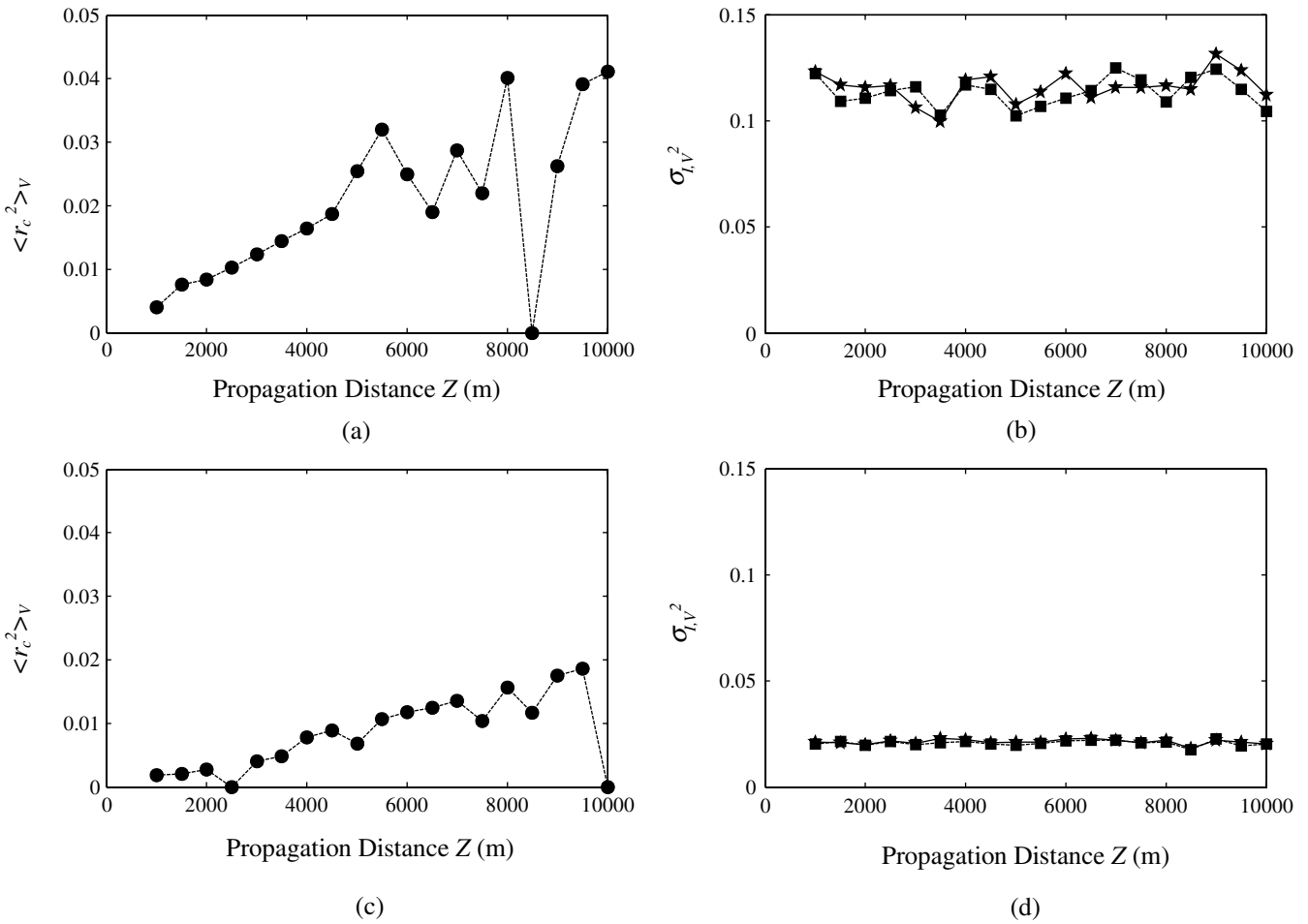

Fig. 1 False beam wander variance $\langle r_c^2 \rangle_V$ (a) and (c) and false on-axis intensity variance $\sigma_{I,V}^2$ (b) and (d) induced by the PCB WOS approach. The coherence length is $l_c = 2$ cm (a) and (b) and 5 cm (c) and (d). Tracked (■) and untracked (★) beam results are shown. Other link parameters are listed in Table 1.

Limiting the number of PCB phase screens ($N_{PS} = 30$) when performing the turbulence simulations saves computation time but introduces additional fluctuations in the results, especially when l_c is relatively small. To compensate for this effect, we simulate propagation through vacuum and calculate the beam wander variance $\langle r_c^2 \rangle_V$ and scintillation index $\sigma_{c,V}^2$ that are purely caused by the limited number of PCB screens. To illustrate the magnitude of these errors, Fig. 1 presents vacuum results for $l_c = 2$ and 5 cm. The false beam wander variance increases roughly in a linear fashion with propagation distance but the false scintillation index for both tracked and untracked beams tends to be independent of Z. The values are larger for the shorter coherence length. In the next section we define how corrections are implemented to compensate for the effects of using a limited number of PCB screens.

4 Analytic and WOS Results

In this section we present examples of analytic and WOS beam size, beam wander, and scintillation index results. However, a few example irradiance profiles are first presented to illustrate the characteristics of an average PCB propagated through turbulence. Figure 2 shows analytic tracked (ST) and untracked (LT) profiles created with Eqs. (13) and (14) and corresponding WOS results. In general, the profiles are Gaussian in shape and the tracked beams have higher peak intensities than the untracked beams. These examples also illustrate the close match between the analytic and WOS results. We reiterate that all the results in this section assume the beam is being focused for the indicated propagation distance.

4.1 *Beam Size*

The analytic expressions for LT and ST average beam sizes are given in Eqs. (10) and (11). For the WOS results, the first step in finding the LT beam size is averaging the two-dimensional intensity profiles produced by the 500 turbulence realizations and measuring the e^{-2} irradiance radius. This gives an initial estimate of the beam size $W_{LT,S,0}$. The beam size corrected for effects of a limited number of PCB screens is given by

$$W_{LT,S} = \sqrt{W_{LT,S,0}^2 - \langle r_c^2 \rangle_V}. \tag{23}$$

The false beam wander value $\langle r_c^2 \rangle_V$ in Eq. (23) is the RMS beam centroid variance calculated from a set of vacuum propagations performed with the identical PCB screens used in the turbulence propagations. On the other hand, the ST beam

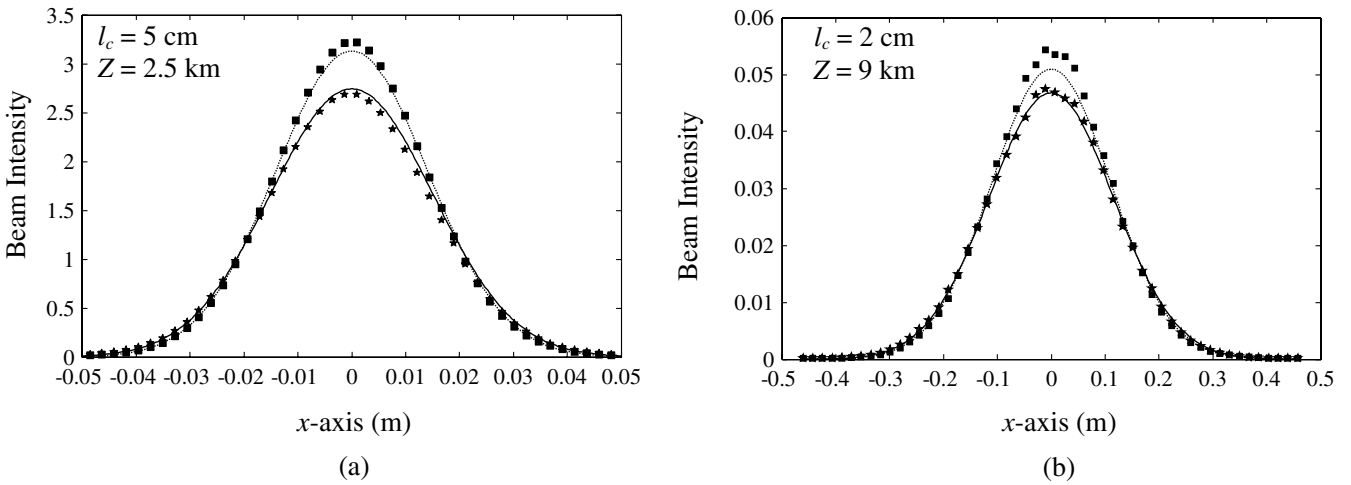

Fig. 2 Tracked (■ and —) and untracked (★ and —) beam intensity profiles for $C_n^2 = 10^{-15}$ m$^{-2/3}$ and (a) $l_c = 5$ cm, $Z = 2.5$ km; (b) $l_c = 2$ cm, $Z = 9$ km. Markers denote WOS results and lines denote analytical results. $F = Z$ and other link parameters are as listed in Table 1.

size, $W_{ST,S}$ is found by first translating each beam in the turbulence propagation set so the centroid is in the center of the numerical grid. The beam irradiance patterns are averaged and the e^{-2} irradiance radius is found. Any additional centroid motion due to the limited number of PCB screens is also removed in the processing, so no correction is applied to the $W_{ST,S}$ values.

Analytic and WOS beam size results are presented in Fig. 3. As expected, the beam size increases with propagation/focus distance, stronger turbulence, and smaller coherence length.

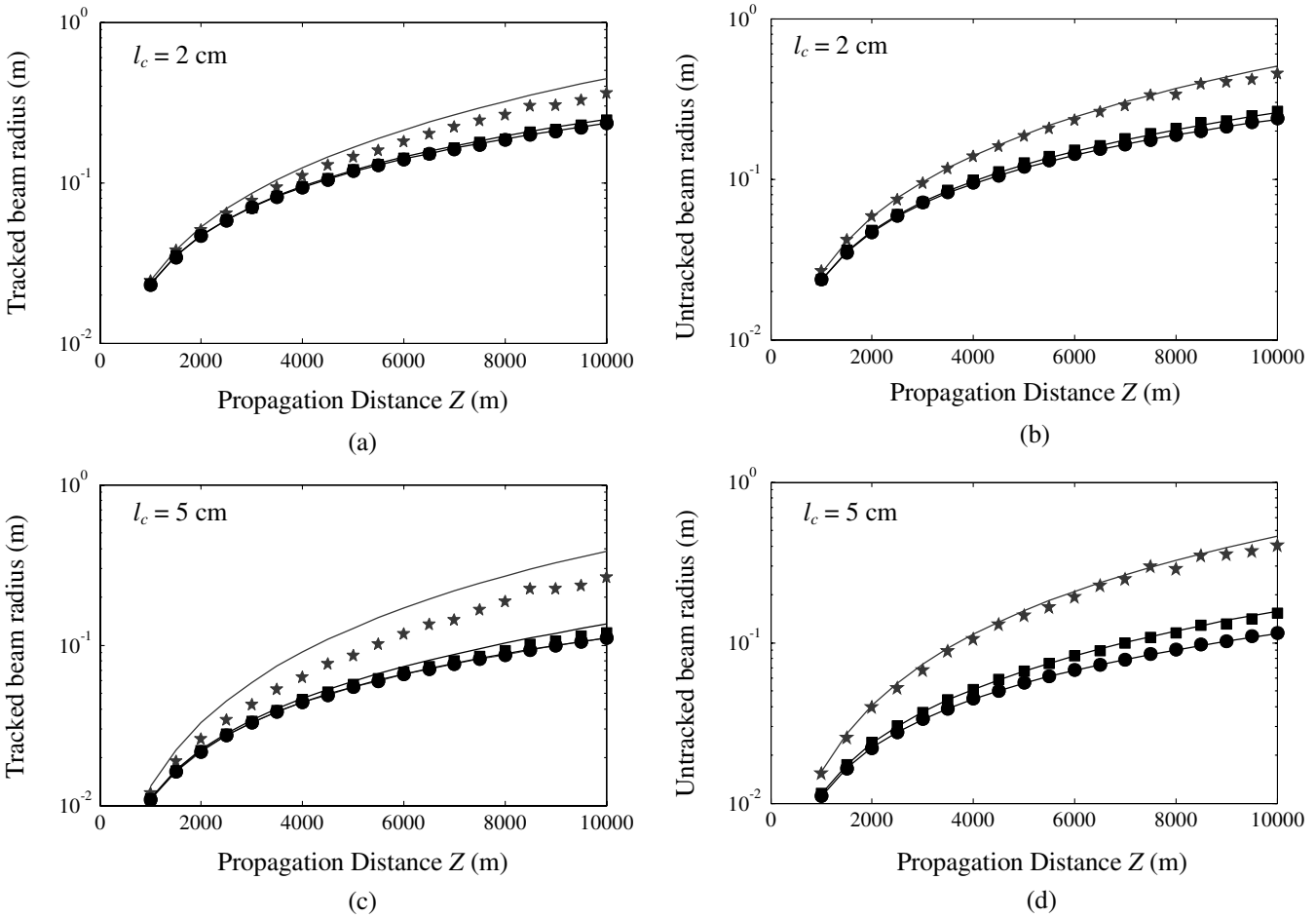

Fig. 3 Tracked (left) and untracked (right) beam size results as a function of Z for $l_c = 2$ cm (top) and 5 cm (bottom). Analytic results are solid lines and WOS results are indicated with markers. Turbulence strength: $C_n^2 = 10^{-14}$ m$^{-2/3}$ (★), 10^{-15} m$^{-2/3}$ (■), and 10^{-16} m$^{-2/3}$ (•). $F = Z$ and other link parameters are given in Table 1.

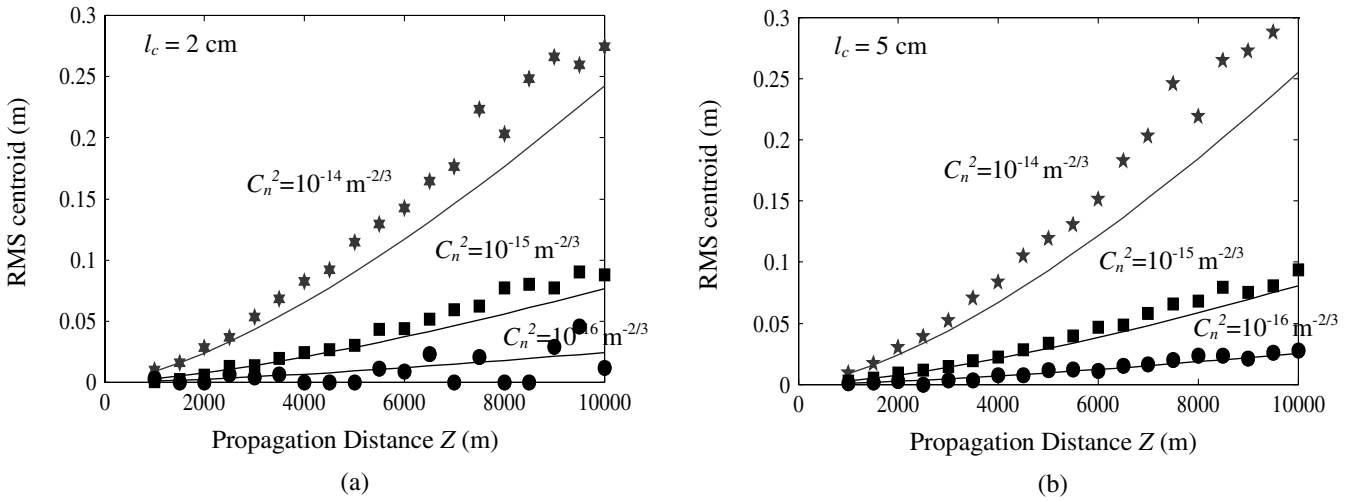

Fig. 4 RMS centroid position (beam wander) as a function of Z for $l_c = 2$ cm (a) and 5 cm (b). Analytic results are solid lines and WOS results are indicated with markers. Turbulence strength: $C_n^2 = 10^{-14}\text{m}^{-2/3}$ (★), $C_n^2 = 10^{-15}\text{m}^{-2/3}$ (■), and $C_n^2 = 10^{-16}\text{m}^{-2/3}$ (•). $F = Z$ and other link parameters are given in Table 1.

The analytic and WOS results are consistent in all cases for the turbulence strengths of $C_n^2 = 10^{-16}$ and 10^{-15} m$^{-2/3}$. For the stronger turbulence case of $C_n^2 = 10^{-14}$ m$^{-2/3}$ and with the tracked beam, the analytic prediction has somewhat higher values than the WOS results.

4.2 *Beam Wander*

The analytic beam wander result is given in Eq. (7). The corrected WOS result $\langle r_c^2 \rangle_S$ is obtained via

$$\langle r_c^2 \rangle_S = W_{\text{LT},S}^2 - W_{\text{ST},S}^2. \tag{24}$$

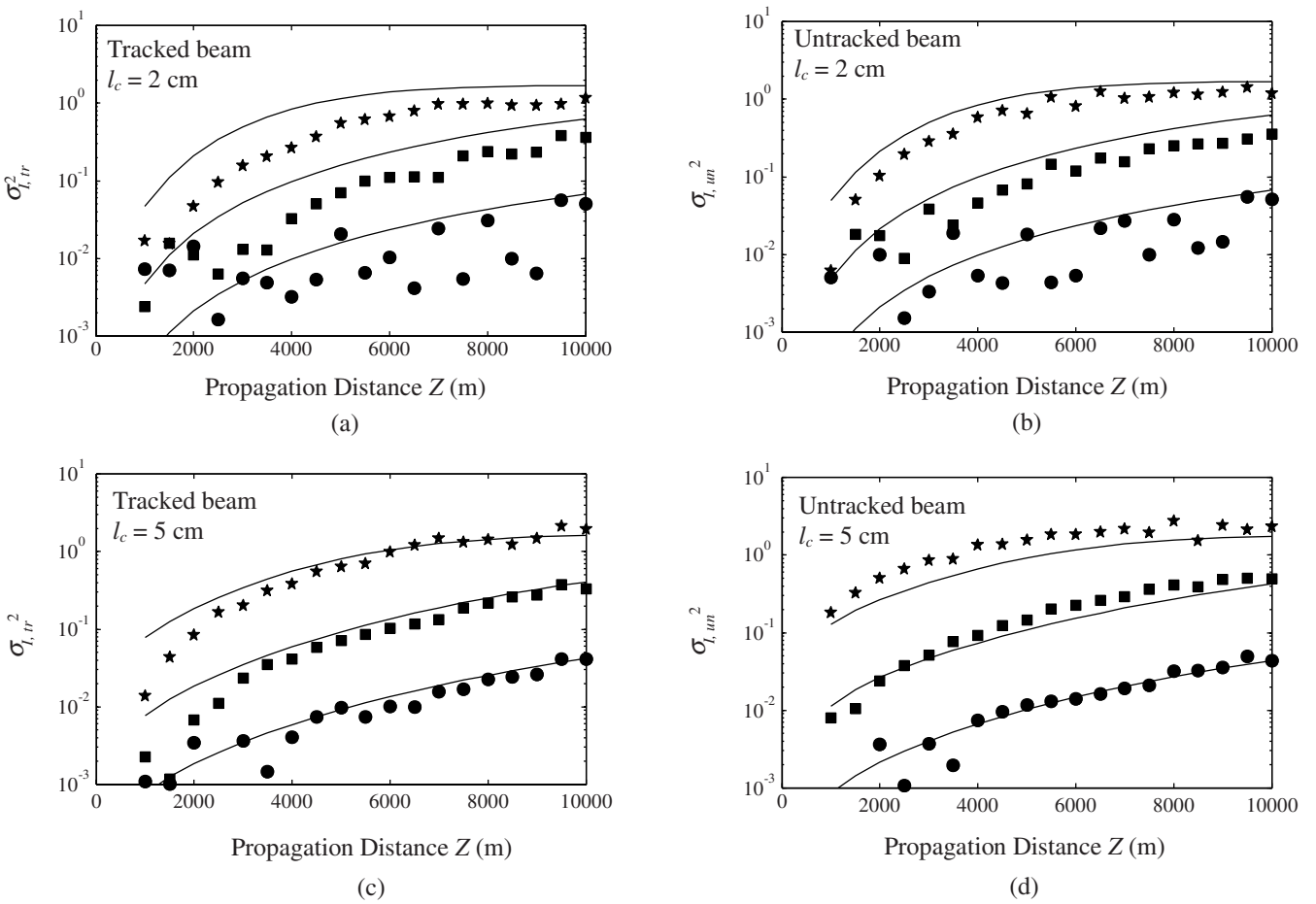

Fig. 5 On-axis scintillation index as a function of Z for tracked (left) and untracked (right) beams and $l_c = 2$ cm (top) and 5 cm (bottom). Analytic results are solid lines and WOS results are indicated with markers. Turbulence strength: $C_n^2 = 10^{-14}$ m$^{-2/3}$ (★), $C_n^2 = 10^{-15}$ m$^{-2/3}$ (■), and $C_n^2 = 10^{-16}$ m$^{-2/3}$ (•). $F = Z$ and other link parameters are given in Table 1.

Figure 4 shows comparisons of the analytical and WOS results. The wander increases with propagation/focus distance and also with turbulence strength. Dependence on the coherence length l_c is weak for the cases presented. The analytic and WOS results are generally consistent, although the WOS tends to produce slightly larger beam wander values. This trend is most obvious in the strong turbulence case ($C_n^2 = 10^{-14}$ m$^{-2/3}$) at longer propagation/focus distances.

4.3 *Scintillation Index*

The analytic scintillation index expressions (on-axis) for tracked and untracked beams are given in Eqs. (21) and (22). For the WOS, the scintillation index is found by computing the normalized variance of the irradiance at the center of numerical grid (optical axis) for the 500 turbulence realizations. Again, the tracked results include the translation of the beam to remove the centroid wander. To compensate for the effects of the finite number of PCB phase screens, the following is used:[23]

$$\sigma_{I,S}^2 = \frac{\sigma_{I,S,0}^2 - \sigma_{I,V}^2}{1 + \sigma_{I,V}^2}, \tag{25}$$

where $\sigma_{I,S,0}^2$ is the initial scintillation index computed from the WOS results, $\sigma_{I,V}^2$ is the false index computed for vacuum propagations with only the PCB phase screens applied, and $\sigma_{I,S}^2$ is the corrected scintillation index.

Figure 5 presents the scintillation results. In general, the index values increase with distance and turbulence strength. The WOS values generally follow the analytic results, although there is clearly more scatter in the WOS points for the $l_c = 2$ cm cases. This is likely due to imperfect correction for the limited number of PCB screens. Saturation of the index value is evident at longer distances for the stronger turbulence cases. We note that for increasing distance beyond that shown in Fig. 5, and therefore increasing Rytov variances, the focused PCB index values appear to peak and then reduce to a saturation value in a way that is similar to results for coherent beams.[31] We expect the saturation regime for a PCB to occur at larger Rytov variances than for a comparable coherent beam.[18] However, further study of this regime would likely require: (1) inclusion of a finite inner scale in the turbulence spectrum, as the scintillation index is highly sensitive to the inner scale; and (2) the exploration of WOS approaches that accurately model the strong fluctuation regime, likely involving high densities of grid points and turbulent screens.

5 Conclusion

The extension of coherent beam wander theory to the case of a focused PCB essentially involves the substitution of the beam waist expression that includes the PCB parameters. Comparison of the resulting analytic expressions for beam size, beam wander, and on axis-scintillation index with WOS results indicates that the GO approximation used in the coherent theory appears reasonable for the PCB theory, at least for most of the link values we studied. The WOS results required corrections for errors caused by the use of a limited number of PCB phase screens. Differences between the analytic and WOS results were primarily seen in stronger turbulence situations. The differences could be due to the use of the Rytov approximation in the analytic derivations but also to numerical issues in the WOS—for example, incomplete correction of the error due to the limited number of PCB screens.

Acknowledgments

This work was supported by the Air Force Office of Scientific Research under the Sensing, Surveillance, and Navigation program, grant FA9550-09-1-0616.

References

1. F. Dios et al., "Scintillation and beam-wander analysis in an optical ground station-satellite uplink," *Appl. Opt.* **43**(19), 3866–3873 (2004).
2. L. C. Andrews et al., "Strehl ratio and scintillation theory for uplink Gaussian-beam waves: Beam wander effects," *Opt. Eng.* **45**(7), 076001 (2006).
3. D. H. Tofsted, "Outer-scale effects in beam-wander and angle-of-arrival variances," *Appl. Opt.* **31**(27), 5865–5870 (1992).
4. P. Beckmann, "Signal degeneration in laser beams propagated through a turbulent atmosphere," *Radio Sci.* **69D**(4), 629–640 (1965).
5. G. A. Andreev and E. I. Gelfer, "Angular random walks of the center of gravity of the cross section of a diverging light beam," *Radiophys. Quantum Electron.* **14**(9), 1145–1147 (1971).
6. R. L. Fante, "Electromagnetic beam propagation in turbulent media," *Proc. IEEE* **63**(12), 790–811 (1975).
7. J. H. Churnside and R. L. Lataitis, "Wander of an optical beam in the turbulent atmosphere," *Appl. Opt.* **29**(7), 926–930 (1990).
8. G. J. Baker and R. S. Benson, "Gaussian-beam weak scintillation on ground-to-space paths: compact descriptions and Rytov-method applicability," *Opt. Eng.* **44**(10), 106002 (2005).
9. L. A. Chernov, *Wave Propagation in a Random Medium*, Dover, New York (1967).
10. V. L. Mironov and V. V. Nosov, "On the theory of spatially limited light beam displacements in a randomly inhomogeneous medium," *J. Opt. Soc. Am.* **67**(8), 1073–1080 (1977).
11. R. J. Cook, "Beam wander in a turbulent medium: an application of Ehrenfest's theorem," *J. Opt. Soc. Am.* **65**(8), 942–948 (1975).
12. H. T. Eyyuboglu and C. Z. Cil, "Beam wander of dark hollow, flat-topped and annular beams," *Appl. Phys. B* **93**(2–3), 595–604 (2008).
13. C. Z. Cil et al., "Beam wander characteristics of cos and cosh-Gaussian beams," *Appl. Phys. B* **95**(4), 763–771 (2009).
14. G. P. Berman, A. A. Chumak, and V. N. Gorshkov, "Beam wandering in the atmosphere: the effect of partial coherence," *Phys. Rev. E* **76**(5), 056606 (2007).
15. L. C. Andrews and R. L. Phillips, *Laser Beam Propagation through Random Media*, SPIE Press, Bellingham, WA (2005).
16. J. Recolons, L. C. Andrews, and R. L. Phillips, "Analysis of beam wander effects for a horizontal-path propagating Gaussian-beam wave: focused beam case," *Opt. Eng.* **46**(8), 086002 (2007).
17. D. K. Borah and D. G. Voelz, "Spatially partially coherent beam parameter optimization for free space optical communications," *Opt. Exp.* **18**(20), 20746–20758 (2010).
18. O. Korotkova, L. C. Andrews, and R. L. Phillips, "Model for a partially coherent Gaussian beam in atmospheric turbulence with application in LaserCom," *Opt. Eng.* **43**(2), 330–341 (2004).
19. L. Mandel and E. Wolf, "Radiation from sources of any state of coherence," in *Optical Coherence and Quantum Optics*, Cambridge University, pp. 229–337 (1995).
20. J. Recolons, L. C. Andrews, and R. L. Phillips, "Analysis of beam wander effects for a horizontal-path propagating Gaussian-beam wave: focused beam case," *Opt. Eng.* **46**(8), 086002 (2007).
21. H. T. Eyyuboğlu, Y. Baykal, and E. Sermutlu, "Convergence of general beams into Gaussian intensity profiles after propagation in turbulent atmosphere," *Opt. Commun.* **265**(2), 399–405 (2006).
22. J. C. Ricklin and F. M. Davidson, "Atmospheric turbulence effects on a partially coherent Gaussian beam: implication for free-space laser communication," *J. Opt. Soc. Am. A* **19**(9), 1794–1802 (2002).
23. O. Korotkova, L. C. Andrews, and R. L. Phillips, "The effect of partially coherent quasi-monochromatic Gaussian beam on the probability of fade," *Proc. SPIE* **5160**, 68 (2004).
24. R. Rao, "Statistics of the fractal structure and phase singularity of a plane light wave propagation in atmospheric turbulence," *Appl. Opt.* **47**(2), 269–276 (2008).
25. S. M. Flatte and J. S. Gerber, "Irradiance-variance behavior by numerical simulation for plane-wave and spherical-wave optical propagation through strong turbulence," *J. Opt. Soc. Am. A* **17**(6), 1092–1097 (2000).
26. M. C. Roggemann and B. Welsh, *Imaging Through Turbulence*, Chap. 3, pp. 57–122, CRC Press, Boca Raton, FL (1996).

27. X. Xiao and D. Voelz, "On-axis probability density function and fade behavior of partially coherent beams propagating through turbulence," *App. Opt.* **48**(2), 167–175 (2009).
28. D. Voelz,Partial coherence simulation, Chap. 9 *Computational Fourier Optics*, pp. 169–189, SPIE Press, Bellingham, WA (2011).
29. X. Xiao and D. Voelz, "Wave optics simulation approach for partial spatially coherent beams," *Opt. Exp.* **14**(16), 6986–6992 (2006).
30. J. Schmidt, *Numerical Simulation of Optical Wave Propagation With Examples in MATLAB*, pp. 149–184, SPIE Press, Bellingham, WA (2010).
31. H. T. Eyyuboglu, "Annular, cosh and cos Gaussian beams in strong turbulence," *Appl. Phys. B* **103**(3), 763–769 (2011).

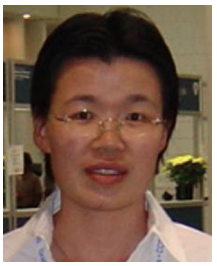

Xifeng Xiao received her BS and MS degrees in physics from Xiamen University, Fujian, China, in 1998 and 2001, respectively. She earned her MS and PhD degrees in electrical engineering in 2004 and 2008, respectively, from New Mexico State University, where she is currently a research assistant professor. Her main research includes simulation and modeling of free-space laser communication, liquid-crystal polarization, acousto-optic imaging spectrometer design, and polarimetric imaging.

David G. Voelz is a professor of electrical engineering at New Mexico State University. He received his BS in electrical engineering from New Mexico State University in 1981 and his MS and PhD degrees in electrical engineering from the University of Illinois in 1983 and 1987, respectively. From 1986 to 2001, he was with the Air Force Research Laboratory in Albuquerque, NM. His current research interests include spectral and polarimetric imaging, laser imaging and beam projection, laser communications, adaptive optics, and astronomical instrumentation development.